
Numerical analysis on the agglomeration behavior of fine particles in plane jet

Min Guo^{1, a}, Jia Li², Xin Su¹ and Guirong Yang¹

¹ Tianjin Academy of Environmental Sciences, Tianjin, 300191, China;

² The Fourth Research and Design Engineering Corporation of CNNC, China

^a251939587@qq.com

Abstract

The plane turbulent jet is selected as the research object to simulate the aggregation situation of the sub-micron grade fine particles in the plane turbulent jet flow field, analyze the movement of the fine particles in the flow field and the evolution process of the particle size and study the influence of different time, interface volume fraction and St number on the aggregation of the fine particles through the coupling of large-eddy simulation and particle population balance model. The results show that the fine particles sizes in the pulse-jet development increase gradually and the number density decreases gradually to tend to be stable. The increase of the interface volume fraction has enhanced the interaction degree between the fluid and the particles and the agglomeration result of the fine particles is more significant. The increase of the St number has affected the movement of the fine particles in the flow field and weakened the agglomeration effect of the fine particles.

Keywords

PM_{2.5}; large-eddy simulation; particle population balance model; free molecular coagulation nucleation; plane turbulent jet.

1. Introduction

The study concluded that the hazard of the fine particles on the environment and the human body mainly depends on small size and large quantity. Among the existing fine particle control technologies [1-3], the turbulent agglomeration technology is one of the technology means with strong economical efficiency and practical value. This technology has fully considered the entrainment produced by the turbulent eddy and the following features of the fine particles, used the eddy structure [4] to change the motion trail of the fine particles and guide the fine particles following the eddy to aggregate, collide and gather so as to change them into the particles with larger size to be collected by the dedusting equipment effectively. The two-phase jet mixing flow formed by the combination of the gas-solid two phase flow and plane turbulent jet has the broad applied value in various fields such as environmental engineering and pneumatic transport process.

The author uses the LES (large-eddy simulation) and PBM (particle population balance) model to study the phenomena of collision and agglomeration of micron and sub-micron fine particles in plane turbulent jet and with the combination of the research development of computational fluid mechanics and particle kinetic, stimulates the movement of the fine particles in the flow field and the influence of different time, interface volume fraction and St number on the agglomeration of fine particles.

2. Basic equations and solution methods

2.1 Equations for flow control

The large-eddy simulation divides the instantaneous movement of turbulence into large-scale motion and small-scale motion through filter function. The large-scale motion is solved by direct numerical simulation and the small-scale motion is solved by the corresponding turbulence model. The detailed flow field information and instantaneous characteristic which are closer to the actual situation of turbulent flow can be given.

To filter the Navier-Stokes equation and define the filtered variable as:

$$\bar{\phi}(x, y, t) = \frac{1}{A} \int_A \phi(x', y', t) dx' dy' \quad (1)$$

In the equation, ϕ is the arbitrary variable (such as particle density, mass fraction, etc.). A is calculation elemental area. t is the time. x and y are the coordinate components. Substitute (1) into N-S equation and convection-diffusion equation to obtain the control equation of the large-eddy simulation as shown in the follows:

$$\frac{\partial \bar{\rho}}{\partial t} + \frac{\partial (\bar{\rho} \bar{u}_j)}{\partial x_j} = 0 \quad (2)$$

$$\frac{\partial (\bar{\rho} \bar{u}_i)}{\partial t} + \frac{\partial (\bar{\rho} \bar{u}_j \bar{u}_i)}{\partial x_j} = -\frac{\partial \bar{p}}{\partial x_i} + \frac{\partial}{\partial x_j} \left(\mu \frac{\partial \sigma_{ij}}{\partial x_j} - \tau_{ij} \right) \quad (3)$$

$$\frac{\partial (\bar{\rho} \bar{\phi})}{\partial t} + \frac{\partial (\bar{\rho} \bar{u}_j \bar{\phi})}{\partial x_j} = \frac{\partial}{\partial x_j} \left(D_s \frac{\partial \bar{\phi}}{\partial x_j} \right) + S_\phi \quad (4)$$

In the equation, ρ is the density of fluid, kg/m^3 . \bar{p} is the fluid pressure, pa. \bar{u} is fluid velocity (i, j - represents x, y components), m/s . σ_{ij} is fluid shear stress tensor ($i-1, 2, 3; j-1, 2, 3$). τ_{ij} is sublattice stress tensor ($i-1, 2, 3; j-1, 2, 3$). D_s is effective diffusion coefficient. S_ϕ is source term of the variable $\bar{\phi}$. The sub-grid stress τ_{ij} uses the following model:

$$\tau_{ij} - \frac{1}{3} \tau_{kk} \delta_{ij} = -2\mu_t \bar{S}_{ij} \quad (5)$$

In the equation, δ_{ij} is the Kronecker operato. \bar{S}_{ij} is strain tensor ($i-1, 2, 3; j-1, 2, 3$). μ_t is sub-grid eddy viscosity coefficient which uses Smagorinsky-Lilly model:

$$\mu_t = \rho L_s^2 |S| \quad (6)$$

In the equation, L_s is the sub-grid mixed length and $|S| = \sqrt{2\bar{S}_{ij}\bar{S}_{ij}}$ represents the mode of strain tensor.

2.2 Population balance model (PBM).

The particle population balance model^[5] describes kinetic events such as collision, condensation, fragmentation, condensation/evaporation, nucleation, and deposition of particles in the discrete system and the details of evolution process of the particle scale kinetics can be obtained by the discrete interval method. This paper supposes that the particles are spheres of uniform density and the particle population is divided into eight sub-intervals from Bin-0~Bin-7 according to the particle size from large to small (Bin represents the particle size). And considering the influence of coagulation on the distribution of particle size (coagulation generally refers to the process during which two spherical particles collide and bond together to form a particle with larger size) and the article population balance model governing equation is shown in the following:

$$\begin{aligned} \frac{\partial}{\partial t} [n(V, t)] &= B_{ag,i} - D_{ag,i} \\ \frac{1}{2} \int_0^V a(V-V', V') n(V-V', t) n(V', t) dV' & \\ - \int_0^\infty a(V, V') n(V, t) n(V', t) dV' & \end{aligned} \quad (7)$$

In the equation: $n(V, t)$ is single-digit concentration of the particle with the volume of V , $1/m^3$. $a(V, V')$ is the coagulation nucleation of the two particles with volumes as V and V' . $B_{ag,i}$ is the coagulation generation (to avoid repeated measurements, please handle with a factor of $1/2$); $D_{ag,i}$ is the coagulation missing term.

The turbulence aggregation is mainly produced by the collision between the particles because of the accumulation of part of particles or maldistribution of radial velocity between the particles caused by velocity contrast produced by the turbulence of gas phase. The main factor affecting the turbulence aggregation is St number (Stokes number) and the interface volume fraction. Among them, Stokes number refers to the ratio of the aerodynamic reaction time of the particle to the time scale of the fluid characteristic and represents the diffusion ability non-dimensional number of the particles in the fluid. The interface volume fraction refers to the volume percentage for the inlet particle under a certain St number. The research shows that the particle size of the fine particles of the combustion source is 95% and distributed in the range of $0.021\mu m$ - $0.2\mu m$. After the calculation, $St \leq 0.1$, that is, belongs to the finite inertia particle. This paper uses the free molecular condensation nuclear model for the simulation [6].

The equation for St is as follows:

$$St = \frac{\tau_p}{\tau_k} = \frac{\rho_p d_p^2 U}{18\mu H} \quad (8)$$

The equation for free molecular condensation nuclear is as follows:

$$a(d_i, d_j) = \frac{2k_B T (d_i + d_j)^2}{3\mu d_i d_j} \quad (9)$$

In the equation: H -is the nozzle height, mm; U -is the inlet main flow velocity, m/s; τ_p is the particle aerodynamic reaction time, ms; τ_k is the time scale associated with large-scale coherent vortex, ms; ε is turbulent energy dissipation rate; Among them, μ is the fluid viscosity, $kg / (m \cdot s)$; ρ_p is the particle density, kg / m^3 ; d is the particle size (i, j - are particles with the first two sizes before the coagulation), μm ; T - is the particle phase temperature, K; k_B is the Boltzmann constant, μ is the continuous phase viscosity, $kg / (m \cdot s)$.

3. Physical model and experimental verification

3.1 Physical Models and boundary conditions

Fig 1 is the structure diagram for the two-dimensional plane turbulent jet and to verify the accuracy and feasibility of the model, the geometric parameters and operating conditions of the model are consistent with the literature [7], that is, taking flow direction length (X) \times length (Y) = $96H \times 68H$, nozzle height $H = 10mm$, injecting the gas-solid two-phase flow into the rectangular space with $U = 10m / s$, defining the characteristic time scale $T_0 = H / U$, taking the calculation time step as $0.001s$ and letting the inlet Reynolds number Re meet:

$$Re = U \bullet \frac{2H}{\nu} = 11300$$

The particle phase density = 1000kg/m^3 . The structured staggered mesh is used to disperse the computational region and the SIMPLE program is used to solve the N-S equation and the composition equation. The spatial discretization uses the Quick format.

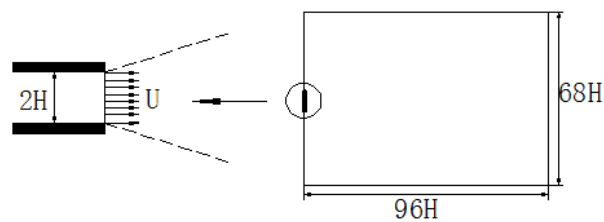


Fig. 1 Structure diagram for the two-dimensional plane turbulent jet

3.2 Experimental verification

Based on the development of the vortex structure from the initial stage to the stable stage of the two-dimensional plane jet flow field at $\text{Re}=11300$, the three stages of jet development are the initial, middle and stable stages of the jet development and the flow field characteristics of each stage are fitted well with the simulation results of Jin Yuhui et. al^[7]. When $T=40T_0\sim 160T_0$, there is the symmetric spanwise vortex with opposite rotate direction at the upper and lower shear layers of the jet at the initial stage. With the development of the spanwise vortex, the vortex interacts with each other and gradually forms a staggered distribution state, resulting in the third vortex created between the two vortices and producing the "cat eye" structure similar to that in the mixed layer flow. When $T=200T_0\sim 240T_0$ at the mid-term of jet development, the small vortex gradually develops large. The downstream small vortex and the upstream subsequent vortex are gradually entrained by the large vortex and the size of the large vortex increases continuously with the pairing and coalescence by the large vortex. During this process, there is even the "three-pole" phenomenon of the synchronous pairing of the three vortices. When $T\geq 280T_0$, under the continuous pairing and coalescence of the large vortex, these vortex pairs interact with each other to gradually get away from the center line and generate the staggered eddy structure with larger size and then gradually reach the stable state.

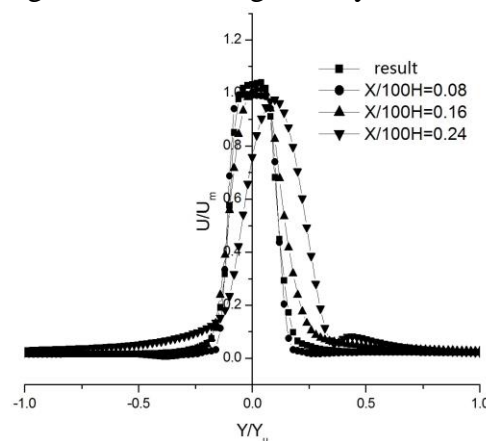


Fig. 2 Self-similarity of flow velocity

According to the statistical method of the literature^[7], the low velocity distribution of the sections with different features are taken to define the U_m as the flow velocity on the center line of the jet and the Y_u as the distance of the velocity of the 1/2 to the velocity of the center line and to nondimensionalize the axial parameters of the X, Y . As shown in the Figure 3, the flow velocity distribution on the section of $X/100H=0.08, 0.16$, and 0.24 reflects that the flow field has good self-similarity, which is consistent well with the experimental results and shows the feasibility of this model for the plane mixed jet simulation.

4. Simulation results and analysis

4.1 Influence of vortex structure on particle agglomeration

Taking the initial particle size as $\text{Bin}7=0.3\mu\text{m}$, St as 10-3, fluid inlet Reynolds number Re as 11300 and inlet particle volume fraction as 5×10^{-4} , this section selects the vortex structure in the jet space when the dimensionless time $T=300T_0$.

Figure 3(a) and (b) are the jet vorticity distribution diagram and the detailed view of the vorticity contour line and it can be seen from the 4(a) that the jet are in the vortex street structure similar to the Karman(Karman Vortex Street) at $T=300T_0$. In the downstream of the jet, the small vortex develops to large vortex gradually and tends to be stable and the vorticity intensity gradually weakens. There is the symmetric vortex pairing structure with opposite flow direction in the upper and lower shear layers at the bottom of the jet, which was also confirmed in the literature^[8]. The aggregation of the fine particles in jet space at $T=300T_0$ has been analyzed in the following.

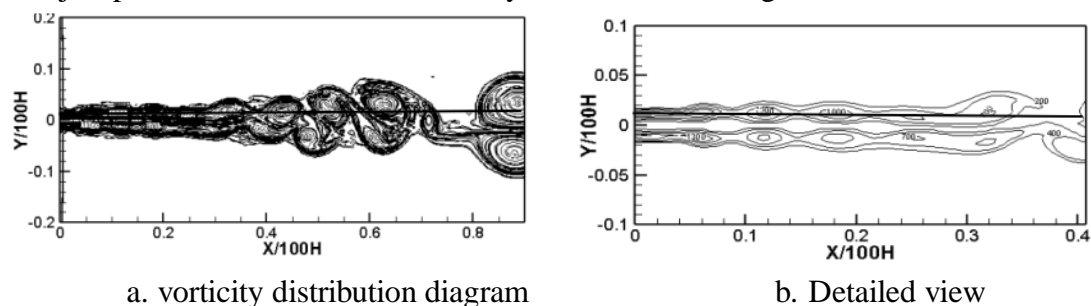
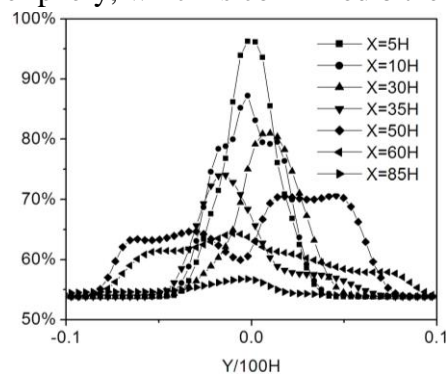


Fig. 3 Detailed view distribution of the jet space vorticity field and the vorticity contour line

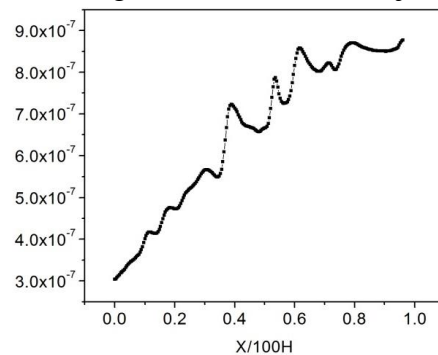
The literature^[9] pointed out that the existence of vortex has important influence on the motion distribution of the particles and high vorticity intensity has enhanced the entrainment of the vortex and improved the probability of local collision coagulation of the particles. Taking the $Y=H$ as the characteristic interface, the Figure 4(a) monitors the size changes on the flow direction and finds that the size tends to increase in fluctuation manner, that is, there are peaks and valleys. Combining the Figure 3(a), it can be found that the valley is in the outer edge of the vortex region while the peak value basically in the vortex region of the flow field. It can be known that the most of the particles with larger sizes are generated in the vortex region, indicating that the existence of the vortex and the better following feature of the fine particles cause the local aggregation of the particles in the vortex region and the particles with larger sizes have better effect of agglomeration among the particles.

With the combination of the Figure 3 (a), the ($X = 5H, 10H, 30H, 35H, 50H, 60H, 85H$) with different features in the direction perpendicular to the flow direction is taken to get the volume fraction changes of the three small, medium and large sizes of ($\text{Bin}7, \text{Bin}5, \text{Bin}1$) along the flow direction and get the graphs (b), (c), and (d), respectively. From the (b), it can be seen that the volume fraction of the particles is in parabola type in the Y direction at $X=5H$ and except for part diffused particles, most of the particles moves with the jet. There is the symmetric vortex structure with opposite flow direction in the upper and lower shear layers of the jet at $X=10H$ and the small particles are featured by small mass and strong diffusion ability. Part of the small particles are aggregated and the aggregation of part of them is enhanced with the increase of volume fraction. There is saddle on both sides of the wave peak. The literature^[10] has confirmed the above. With the combination of Figure (c) and (d), it can be seen that the volume fraction of $\text{Bin}7$ with the size of $\text{Bin}5$ gradually decreases and the volume fraction of $\text{Bin}1$ increases, showing that part of the aggregated smaller particles collide and aggregate into larger particles, leading to decrease in volume fraction of the small particles and increase in volume fraction of larger particles. With the deepening influence between the vortex, the wave peak of $35H$ starts to deviate the medial axis at $X=30H$, which is consistent with the development of the flow field where the symmetrical vortex structure gradually deviates the center line and reflects the influence of vortex structure on the local aggregation of the fine particles. Moreover, the volume fraction of $\text{Bin}7$ further

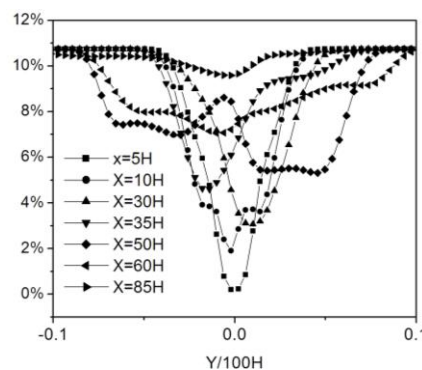
decreases and the volume fraction of the large particles further increases in Figure 4(b). At the same time, the peak curve changes from high to short, showing that the range of local aggregation is enlarged correspondingly with the vortex movement. Taken together, the jet vortex structure has further enhanced the local aggregation and collision effect between the particles to some extent. There is paring and aggregation of the original vortex at $X=50H$ to generate large-scale vortex, which can enhance the perturbation action on the flow field. The vortex paring and aggregation increases the aggregation of the particles at the center line and the aggregation effect is significant, resulting in the double-peak structure. When $X=60H, 85H$, there are further increased vortex scale, weakened intensity, increased particle inertia, decreased interaction of the vortex, poor aggregation effect, slow increase of volume fraction of the larger particles and outflow of most part of them, which shows that the particle aggregation is closely related to the particle diffusion characteristics and gas phase turbulence. Meanwhile, it is found that in the flow process, the number density of particles is increased from the center of the jet to the periphery, which is confirmed by the results of Liu Yinhua et al. [11].



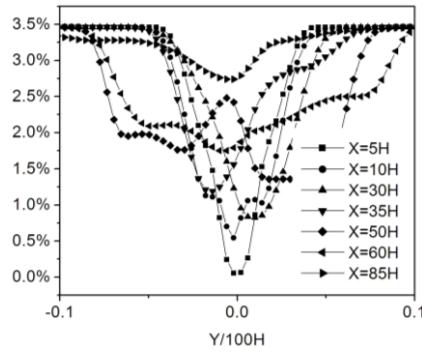
(a) Particle size changes in the direction of jet flow direction



(b) Volume fraction changes of Bin7 (small particle size) in the direction of flow direction



(c) Volume fraction changes of Bin5 (medium particle size) in the flow direction



(d) Volume fraction changes of Bin1 (large particle size) in the flow direction

Fig 4 (a)~(b): particle size changes in the flow direction and particle volume fraction changes on the sections with vertical flow direction

Figure 5 and Figure 6 show the particle size change with time and evolution of particle number density with time. With the time and development of the flow field, the size increases gradually and tends to be stable and the number density gradually decreases and tends to be stable, which indicates that under the action of the plane turbulent jet flow field, the fine particles collide and aggregate with the vortex aggregation to gradually coalesce to be the larger particles and decrease the number density of the particles.

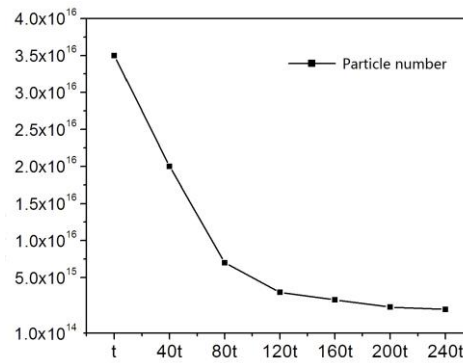
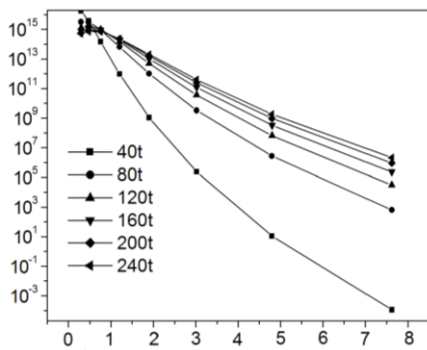


Fig 5 Particle size changes with time Fig 6: Evolution of particle number density over time

4.2 Influence of St number on the agglomeration of fine particle

Taking $Re=11300$ and inlet particle volume fraction as 5×10^{-4} , the Stokes numbers are simulated as 1×10^{-3} , 5×10^{-3} , 1×10^{-2} , 1.5×10^{-2} , 2×10^{-2} , respectively and the flow field at $T=280T_0$ has been fully developed. Figure 7 shows the volume fraction change of the inlet particles with the initial particle size at $T = 280T_0$ in the flow direction. With the increase of St number, the volume fraction of the particles with initial particle size of the jet flow field has decreased and the aggregation effect is getting weak with gradual decline. When $St=1 \times 10^{-3}$, the volume fraction decreases rapidly with large variation range and the small particle agglomeration effect is significant. Same to the change tendency of curve $X=5H$ in Figure. 4(b), due to the small initial fine particle size, good followability and faster response to the flow field, the entrainment and aggregation effect of the particles is good. Meanwhile, there are much more particles with small size in the jet flow field to make the local aggregation remarkable and further improve the aggregation effect of particles with larger size. When the St number increases, the particle size increase during particle agglomeration gradually slows down, indicating that the increase of particle size enhances the inertial force of the particles and the response to the flow field is weakened, resulting in that the larger particles are easy to be out of the vortex to flow to the downstream. There are less particles in the jet flow field, which has weakened the interactions between the fluid and the particles and reduced the aggregation and agglomeration effect of the particles with

the vortex gradually. This result has been also confirmed by the gentle change tendency of volume fraction of the curve $X=60H$ in Figure. 4(b).

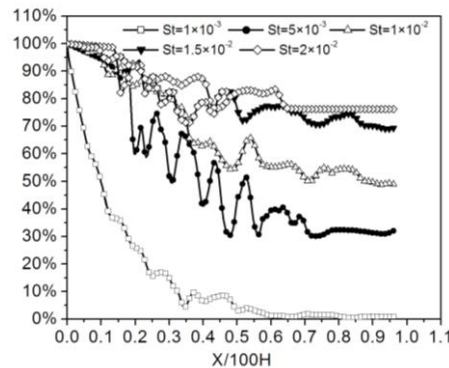


Fig 7 volume fraction changes of initial particle in the flow direction at $T=280T_0$

5. Conclusion

Combining the local aggregation of micron and submicron fine particles in the large-eddy simulation and population balance model simulation in the plane turbulent jet process, this paper has studied the agglomeration effects of fine particles at different times, volume fractions and St numbers. The results show that the fine particles are affected by the vortex structure during the turbulent jet process and the particles with smaller size have good followability to be able to move with the vortex better. There is local aggregation for the fine particles and the probability of collision between particles increases. The particles with larger size have better aggregation effect and with the increase of the size, the particles gradually reverse the effects of turbulence vortex under the action of the centrifugal force, resulting in that the inlet size migrates toward the large particle size. The interaction effect of the fine particles with larger inlet volume fraction and the flow field is significant, which can promote the development of vortex structure in the flow field and improve the agglomeration collision effect of the particles. Particles with smaller St-numbers have stronger diffusion capacity and movement speed, and the degree of response to the flow field is higher, which enhances the effect of local aggregation and collision of the particles. The particle size changes greatly, and with the increase of the St-number, the particle size is in lower growing rate, reflecting that the effect of the flow field on the particles decreases gradually and the response sensitivity is increasingly weakened.

References

- [1] YAN J, CHEN L, YANG L. Combined effect of acoustic agglomeration and vapor condensation on fine particles removal[J]. Chemical Engineering Journal, 2016, 290:319–327.
- [2] LIU Jian-ping. Research progress on agglomeration of fine particles from coal fired flue gas [J]. Shandong chemical industry, 2014, 43 (8): 36-39.
- [3] GE Yang-zhen, LIU Xi-pu, ZHANG Peng-fei, et al. Inhalable particles agglomeration technology [C]// The fifteenth conference of China electric dust collection, Anhui: China Environmental Protection Industry Association, 2013:44-49.
- [4] YE Fei. Unsteady vortex motion and its mechanism [D]. Tianjin :Tianjin University, 2010.
- [5] SU Jun-wei, GU Zhao-lin, XU. discrete phase system population balance model solving algorithm [J]. Chinese Science: Chemistry, 2010, 40 (2): 144-160.
- [6] XU Jun-bo, ZHANG Li, YUE Ren-liang, et al. The computational fluid dynamics simulation of $PM_{2.5}$ fine particle coagulation [J]. computer and applied chemistry, 2013,30 (8):831-834.
- [7] KIM Han-hui. Large eddy simulation of coherent structure of Zhejiang University [D]. Zhejiang: Zhejiang University, 2002.
- [8] LUO Kun, LIU Xiao-yun,, et al. Direct numerical simulation of gas solid turbulent jet with high Reynolds number [J]. Journal of engineering thermal physics, 2004 (3): 431-434.

- [9] ZHANG Peng-fei, MI Jian-chun, PAN Zu-ming. The influence of the arrangement spacing and particle concentration on the turbulent flow of fine particles in the device [J]. proceedings of the China Electrical Engineering, 2016, 36 (6):1625-1632.
- [10] YAN Jie. The direct numerical simulation of the interaction between the and the phase of the three-dimensional gas-solid two-phase flow in a flat plate [D]. Zhejiang: Zhejiang University, 2009
- [11] LIU Yan-hua, FU Jun, ZHANG Kai. Nucleation and coagulation of nano particles in the plane jet field and the Acta Physica Sinica [J]., 2010, 59 (6): 4084-4092.